Agnieszka Pietrzak (Autor)

Realization of High Power Diode Lasers with Extremely Narrow Vertical Divergence

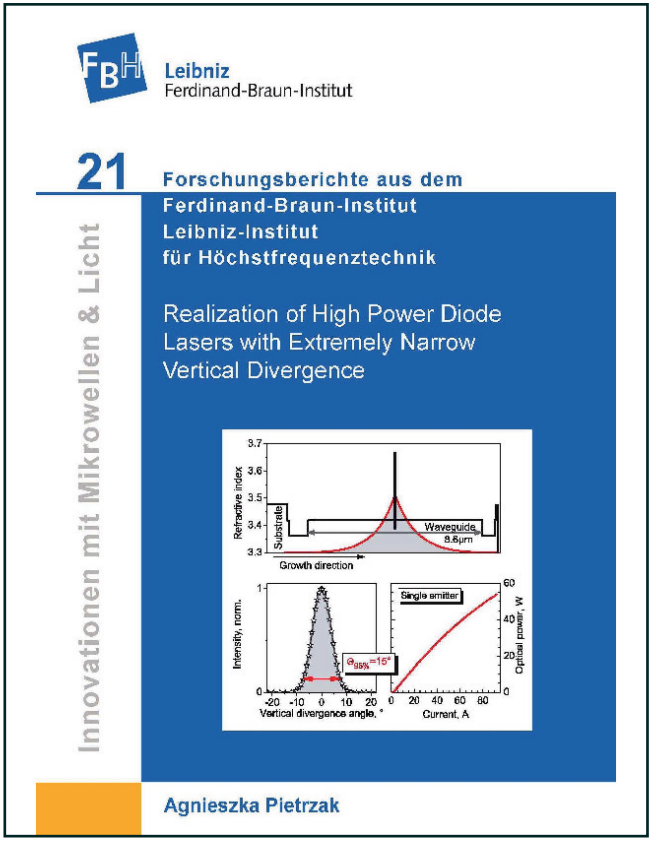

https://cuvillier.de/de/shop/publications/39

1

Introduction and motivation

This work concerns high-power semiconductor diode lasers with emission wavelengths in the range of 1050-1150 nm. Diode lasers typically demonstrate high electrical-to-optical conversion efficiencies at relatively high optical power and cover a wide spectral range. These characteristics, together with their compactness, make them very attractive optical sources for commercial applications. Therefore, diode lasers are currently widely applied in industry as pump sources of solid state laser systems, in direct material processing, in fiber and space telecommunications, and in various medical treatments. Currently, significant diode laser research and development is in progress, aiming on achieving the maximum possible optical power and electro-optical efficiency, together with an improved beam quality. In the future, diode lasers will enable high performance optical systems with reduced overall cost. Table 1 shows the best published results of single emitter laser diodes and table 2 the best commercially available products.

The main aim of this work is the realization of diode lasers which emit high optical power within an extremely small vertical divergence angle (direction perpendicular to the active region). High performance diode lasers, which emit a power above 20 W within a far field angle below 10° (defined as full width at half maximum, FWHM) are sought-after. The focus on the reduction of the vertical divergence angle is dictated by application needs such as easier and more efficient beam shaping, which makes optical systems less expensive. A small vertical divergence angle (containing 95% of the optical power) minimizes the power loss and aberrations during the beam collimation process.

The general concept chosen for the reduction of the vertical far field angle are epitaxial structures based on very wide waveguides which are named Super Large Optical Cavity structures (SLOC) in this work. The SLOC concept is considered mainly due to three reasons. Firstly, the beam divergence can be reduced simply by widening the waveguide. The vertical beam profile has a Gaussian shape and the divergence angle containing 95% optical power is stable up to high carrier injection levels.
Secondly, the SLOC design provides a large equivalent vertical spot-size – the high optical field intensity is distributed over a larger area in the vertical direction. This reduces the risk of optical damage of the internal structure and the laser mirrors (catastrophic optical mirror damage, COMD). Consequently, higher output powers can be emitted before the damage occurs. Thirdly, the advantage of this design is the robust tolerance of the growth of the thick waveguides and claddings. Higher order modes are suppressed in a loss discrimination process by varying the thickness of the claddings, whereby good mode suppression with high tolerance of this thickness is achieved.

The emission wavelength of 1050-1150 nm requires an active region consisting of an $In_x Ga_{1-x} As$ quantum well with high incorporation of indium content ($x = 0.28$ to $x = 0.37$,

respectively). In structures based on thick waveguides, the overlap of the optical mode with the active region is low. In order to obtain high optical gain, the laser structures comprise a multi-quantum well active region where the quantum wells are separated with $GaAs_{1-y}P_y$ barriers. For structures emitting at wavelengths beyond 1100 nm, the material chosen for the waveguides was GaAs. This choice was made for two reasons. Firstly, for the laser structures emitting at longer wavelengths the GaAs waveguide is expected to build a sufficiently high barrier which confines the electrical carriers in the active region. Secondly, the GaAs material features high electrical and thermal conductivity. Therefore, the thick waveguide layers can be lowly doped. A low free carrier density results in low internal absorption loss making the realization of lasers with a longer gain medium possible. For structures emitting at shorter wavelengths than 1100 nm, an $Al_{0.1}Ga_{0.9}As$ waveguide is utilized in order to strengthen the carrier confinement in the active region. The $Al_xGa_{1-x}As$ alloy, however, is characterized by lower electrical and thermal conductivity (due to higher effective mass of the electrons and thus lower mobility). Therefore, in this case higher doping of the waveguide is required. The thick waveguides are embedded in $Al_xGa_{1-x}As$-cladding layers with aluminum contents between 10% and 25%. The aluminum content in the claddings is chosen in a way to obtain a low refractive index step at the waveguide-cladding interface and thus to reduce the number of higher modes in the vertical cavity.

The laser structures optimized for narrow beam divergence angles are processed as broad area single emitters with long (4 - 8 mm) Fabry-Perot optical resonators in order to reduce the thermal and series resistance of the devices. The long gain medium reduces the out-coupling losses and allows the use of low reflectivities of the front facet. Low reflectivity reduces the optical load on the facet and is expected to reduce the risk of COMD. Consequently, higher overall optical output power is expected to be achieved before a failure of the device occurs.

This work involves a theoretical study of the waveguiding and carrier-transport properties of the laser structures and an experimental part dealing with the electro-optical characterization of processed laser devices, intended in part to diagnose what limits the laser performance.

Wavelength	Vertical divergence angle	Maximum optical power, (CW, 25°C)	Maximum wall-plug efficiency	Single emitter geometry, (stripe × length)	Company
915 nm	35° (FWHM)	23 W	65%	90 µm × ---	Axcel Photonics 2008 [1]
940 nm	---	26 W (15°C)	64%	90 µm × 5 mm	Intense 2009 [2]
980 nm	22° (FWHM) 40° (95%)	25 W (15°C)	54%	96 µm × 4 mm	FBH 2009 [3]
975 nm	15° (FWHM) 28° (95%)	11 W	58%	90 µm × 3 mm	FBH 2009 [4]
1060 nm – 1080 nm	31° (FWHM) ~50° (95%)	16 W	74%	100 µm × 2-3 mm	Ioffe 2004 [5]
1150 nm	20° (FWHM) 34.5° (95%)	13 W	53%	100 µm × 4 mm	FBH 2005 [6]
1060 nm	14° (FWHM)	15 W	52%	100 µm × 4 mm	FBH 2008 [7]
1130 nm	13° (FWHM) 20° (95%)	38 W (QCW)	40%	200 µm × 8 mm	FBH 2008 [8]
1060 nm	*8.6°*(FWHM) *15° (95%)*	*12.5 W* *30 W (QCW)*	*27%*	*200 µm × 8 mm*	*in this thesis*

--- - data not available

Table 1.1. The opto-electrical parameters of single emitter prototypes presented in the years 2001-2009. The laser devices are presented in respect to decreasing vertical divergence angles and the emission wavelength range, first 915-980 nm, second 1060-1150 nm.

Company	Wavelength	Vertical divergence angle	Maximum optical power, (CW, 25°C)	Maximum wall-plug efficiency	Single emitter geometry, (stripe × length)
JDS Uniphase	915 nm – 976 nm	27° (FWHM)	10 W	55%	100 µm × ---
Oclaro	915 nm – 975 nm	23° (FWHM)	9 W 11W	>50% >55%	90 µm × 3.6 mm 90 µm × ---
LUMICS	915 nm – 975 nm	27° (FWHM)	12 W	---	95 µm × ---
	1064 nm	30° (FWHM)	11 W	---	190 µm × ---
AXCEL Photonics	1064 nm	30° (FWHM)	3 W	---	100 µm × ---

--- - data not available

Table 1.2. The electro-optical parameters of the currently (October 2011) commercially available single emitters. Emission wavelength: 915 – 1064 nm.

1.1. Overview of chapter contents

Chapter 2: A literature overview of various approaches of the optical mode expansion targeting the reduction of the vertical far-field angle.

Chapter 3: The basic concept of a diode laser with a Fabry-Perot resonator as well as the phenomenological laser model is presented. The software used to simulate the one-dimensional optical mode propagation in a layered media and the vertical far-field distribution of the emitted light is presented.

Chapter 4: The epitaxy process of high-power, 1050 – 1150 nm, diode lasers based on GaAs substrates as well as the technology and packaging of high-power broad-area diode lasers are presented.

Chapter 5: Measurement techniques and experimental setups for the diode laser characterization utilized within this work are presented.

Chapter 6: The results of the one-dimensional simulations of the basic features of the SLOC design are presented. The first results concern the variation of the near- and far-field profile as a function of the optical transverse cavity width. It is further shown that, in the structures based on extremely wide waveguides, the claddings lose their ability to confine the mode and that the multi-quantum well active region exhibits guiding properties. The influence of the active region design (e.g. quantum well number, quantum well thickness, thickness and composition of the barriers) on the mode properties like the confinement factor and on the beam divergence is presented. The study of the mode confinement by the active region leads to an innovation in the far-field angle reduction. The new concept for far-field reduction based on interpolation of low-refractive-index quantum barriers (LIQB) to separate the quantum wells is presented. Moreover, the dependence of the vertical equivalent spot-size on the waveguide thickness and number of QWs is discussed. The methods used for the suppression of higher order transverse modes in SLOC structures are presented.

Chapter 7: Theoretical and experimental studies of limiting factors to the maximum optical power of the diode lasers based on SLOC design are discussed. The study is focused on structures with 3.4 µm thick symmetric waveguides and MQW active regions emitting at 1100 nm. It is shown that one of the factors reducing the peak optical power is vertical carrier leakage and carrier accumulation in the p-type waveguide. Moreover, it is presented that the carrier confinement in the active region can be strengthened by increasing the number of quantum wells in the gain medium. The result of the study is an increase of the optical power from 45 W to 55 W under ‘zero-heat’ conditions.

Chapter 8: This chapter is focused on the further development of high power diode lasers with the simultaneous reduction of the vertical far-field angle. To assure good carrier confinement in the active region, the tested diode lasers utilize a four QW gain medium emitting at a longer wavelength of 1130nm. The far-field narrowing is obtained by increasing the waveguide thickness from 3.4 µm to 5.0 µm. Based on the experimental data, the influence of the laser geometry on the reduction of the electrical and thermal resistance (and thus a further increase of the optical output power) is discussed. The experimental results of diode lasers based on the design with reduced divergence angle

from 18° to 13° (FWHM) and simultaneously maintained high optical output power of more than 35 W are presented.

Chapter 9: This chapter deals with the theoretical and experimental study of high power diode lasers emitting at 1065 nm. Factors deteriorating the internal efficiency and factors limiting the reduction of the vertical divergence angle are discussed. More exactly, the influence of the composition of the $Al_xGa_{1-x}As$ waveguide on the effective barrier depth and on the optical mode distribution is discussed. The reduction of the far-field angle (13° to 10° at FWHM) is realized by widening the $Al_{0.1}Ga_{0.9}As$ waveguide from 6.0 µm to 8.6 µm. The further reduction of the divergence angle, especially the angle containing 95% of the optical power, by widening the waveguide was not successful. The limit to the minimum far-field angle is caused by the high average refractive index of the multi-QW active region.

Chapter 10: In this chapter, it is shown that the use of low refractive index quantum barriers (LIQB) reduces the high average refractive index of the active region and results in a lower divergence angle of the laser beam. Structures based on 8.6 µm thick $Al_{0.1}Ga_{0.9}As$-waveguides with LIQB are considered. Furthermore, the limits of the LIQB design are investigated. High power devices delivering 30 W of quasi-CW optical power enclosed in a beam divergence reduced to 8.6° (FWHM) and 15.4° (95% power content) are demonstrated. Moreover, the lateral beam profiles of the LIQB design are presented in comparison to the SLOC design.

2

Overview of general concepts for vertical mode expansion

The vertical far-field profile is obtained from the Fourier transform of the electric field distribution at the laser surface (near-field) perpendicular to the active region. Therefore, the reduction of the vertical divergence angle of the laser beam is mainly based on the extent of the optical transverse mode. The optical mode is tailored by the refractive indices of the particular epitaxial layers and their thicknesses [1]. In the literature one can find various approaches for the optical mode expansion and, consequently, for the reduction of the vertical far-field angle. Some of them are briefly described below.

2.1. Thin Active Layer (TAL) lasers

The design concerns double heterostructure lasers, i.e. the active layer with low energy band-gap is sandwiched between two high band-gap layers (Figure 2.1.a).The key concept of the TAL structure is a significant reduction of the active region thickness (from e.g. 140 nm to 25 nm) so that most of the optical mode penetrates into the adjacent cladding layers, resulting in a narrower vertical divergence angle (Figure 2.1.b). The drawback of this design is the high threshold current density due to a low confinement factor and the high free-carrier absorption loss caused by the light propagation in the highly doped claddings.
To satisfy the requirements of low divergence and low threshold current a '*thin tapered-thickness active layer*' (T^3 *laser*) is proposed [2]. The very thin active layer (showing quantum properties) is placed near the mirror in order to obtain the narrow vertical divergence angle and is widened in the inner part of the laser (showing bulk material properties) for maintaining high optical mode confinement and thus low threshold current density (Figure 2.1.c.).

The design performance may degrade due to the optical mode instability with increasing injection current caused by induced carrier refractive index change.

The vertical far-field angle of 10° and the optical power of 120 mW are presented in [2] from a 65 µm long laser at a wavelength of 780 nm).

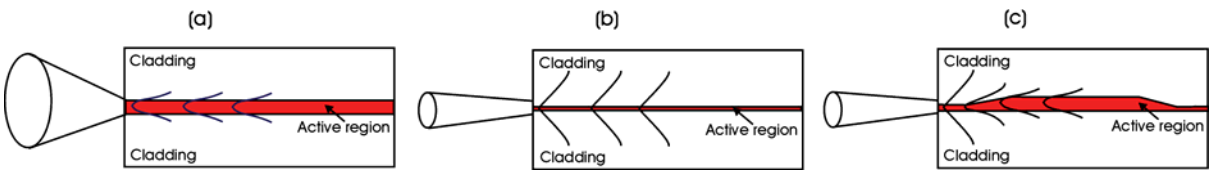

Figure 2.1. The basic concepts of the (a) DH structure, (b) TAL design and (c) T^3 design, redrawn from [2].

H. Kobayashi et al. [3] presented an improved design called '*Tapered thickness MQW waveguide*'. Here, the multi-QW active region is embedded in a tapered shape waveguide. The waveguide helps to confine light in the active region and plays a role of a tapered active layer in the T^3 design where the light is guided. A vertical far-field of 11.8° is reported. The additional waveguide layers, generally low doped, eliminate the free-carrier absorption losses. The main disadvantage of this design is the growth method. The so called Selective Area Growth technique (SAG) has to be used, which is more challenging than the one-step epitaxy.

2.2. Separate Confinement Heterostructure (SCH)

The quantum well (QW) layer is too small to effectively confine the light. To compensate this effect, the active region is embedded between two additional low doped layers (called waveguide or confinement layer) with a lower refractive index than that of the QW and higher than that of the cladding layers. The optical mode is confined in the waveguide by the low refractive index claddings with its maximum intensity in the active region.

SCH with low-index layers

In [1, 4 - 7] a single-QW InGaAs/GaAs/AlGaAs graded-index-SCH structure (GRINSCH) is considered. The reduction of the vertical far-field angle is achieved by the implementation of two low-index layers on both sides of the graded waveguide. The low-index layers strongly confine the optical field in the active region (index guiding effect). The optical mode effective index is simultaneously reduced by the low-refractive index layers to the value close to the refractive index of the claddings. Consequently, due to the index anti-guiding effect, the optical mode spreads into the cladding layers resulting in a strong reduction of the divergence angle.

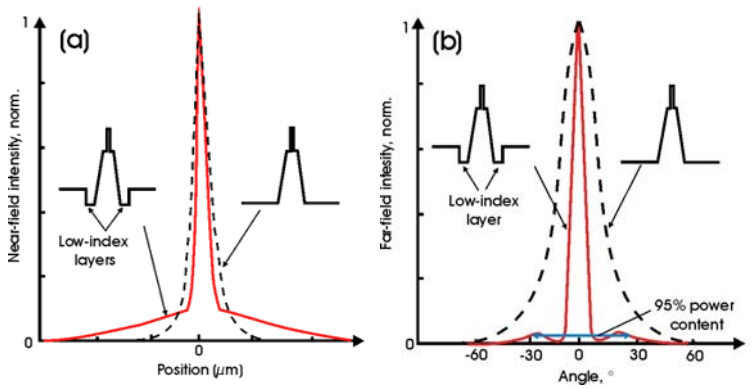

Figure 2.2. The vertical near-field (a) and far-field (b) profiles of the structure with and without low-index layers, redrawn from [4].

Using this design, a vertical far-field angle of 13° (FWHM) and 250 mW of optical power with a slope efficiency of 0.9 W/A from a 2.5 µm-ridge waveguide laser (0.5 mm long) is reported [4]. A. Maląg et al. [8] report 2.4 W optical power emitted into a 13°-14° (FWHM) vertical angle from a 100 µm wide, 1 mm long single-QW laser device (emission wavelength 800 nm).

Although the vertical angle at full width at half maximum is reduced, the design exhibits a far-field with side lobes leading to a wide angle containing 95% of the optical power that is disadvantageous for practical applications.

In order to minimize the optical losses originating from the light propagating in the highly doped p-cladding layer, a structure with only one low index layer at the n-doped waveguide-cladding interface is proposed by Z. Xu et al. [9]. A vertical far-field angle of 12° is reported for this case. An optical power of 500 mW with a slope of 1.0 W/A for a 5 µm-RW laser with cavity length of 1.5 mm is presented in [9] (emission wavelength 808nm).

The same concept is utilized for MQW structures, e.g. [10], where the optical confinement, achieved by the competition of the index guiding and anti-guiding effects, is controlled by the thickness and composition of the low-index layers.

The theoretical analysis of such low-index layer designs emitting at 980 nm results in a predicted vertical far-field angle of 11° (FWHM) [10].

SCH with high-index mode expansion layers – passive waveguide structures

In this design, additional high-index layers (called passive waveguide) in the otherwise low index cladding layers are implemented. The composition and the thickness of the mode expansion layers as well as the distance from the active region are chosen in such way that the optical mode spreads into the cladding layers consistently with a minimum reduction of the light overlap with the active region [11-13]. The idea is presented in the figure 2.3.

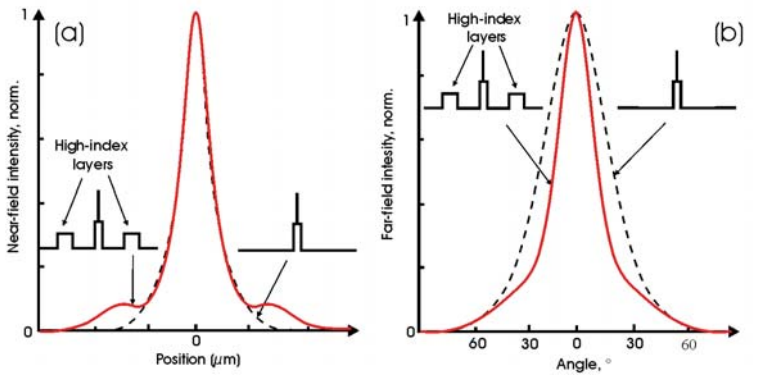

Figure 2.3. The comparison of the calculated (a) near-field and (b) far-field profiles between the SCH structure (black dashed line) and SCH with high-index mode expansion layers (red solid line) [12].

P. M. Smowton et al. [12] report a far-field reduction from 37° to 23° (FWHM) using this structure.

The drawback of this design is the requirement of higher accuracy in the growth process due to very small tolerance regarding the mode-extension layer thickness and composition of the high index layers [12]. In order to improve the growth tolerance B. Qiu et al. [11] propose a structure with a V-profiled (graded) mode-extension layer. Another drawback is that this design does not improve the emission angle containing 95% of optical power. B. Qiu et al. [11] present a reduction of the vertical divergence angle (FWHM) from 26° to 18°. The V-profiled mode-extension is implemented only in the n-type cladding layer in order to avoid the light propagation in the p-doped layer and thus to reduce the optical loss. Using this technology, 380 mW optical power from a ridge waveguide laser is reported. Vakhshoori et al. [14] present a structure (980 nm, InGaAs/GaAsP/InGaP) with 17° vertical divergence angle and 700 mW optical power with a slope of 0.9 W/A from a ridge waveguide laser (3 µm x 750 µm).

The number of high-index layers (or passive waveguides) can be increased. For example, in the work of Y. C. Chen [15] four passive waveguides are symmetrically inserted around the active region, in the cladding layers. The FWHM-vertical divergence is reduced by a factor of four, from 44° (standard SQW GRINSCH) to 11.2°. M. C. Wu et al. [16] present a structure with 16 additional passive waveguides. The 5 µm x 750 µm RW laser emits 620 mW optical power into a vertical far field of 20° (FWHM).

Antiresonant Reflecting Optical Waveguide (ARROW)

The ARROW has its origin in the passive waveguide structures. Choosing the thickness of the high-index layer as odd multiples of $\lambda_1/4$, the antiresonant condition is provided and the layers become highly reflecting (λ_1 is the vertical wavelength in the high-index layer, see the wave-front in figure 2.4, incident under angle Θ) [17-18]. Under such conditions the optical mode is strongly confined and propagates in the low-index layer (in contrast to the conventional waveguides) with embedded active area. To maximize the net reflection, the spacing to the next reflector should also be antiresonant. Therefore, it is chosen as odd multiples of half width of the low index waveguide core [18]. For higher order modes the antiresonant condition is not valid. The high-index layers are transparent for the higher modes and thus they experience large leakage loss. The schematic ARROW structure is presented in figure 2.4 together with mode intensity propagation.
A vertical far-field angle of 18° (FWHM) is reported in [18].

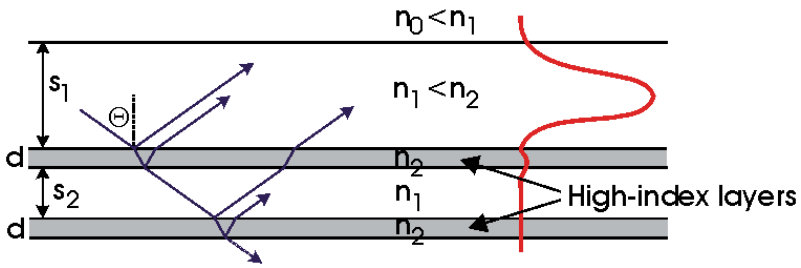

Figure 2.4. The concept of the ARROW structure with the optical mode profile. In the slab s_1 the active region is embedded. Redrawn from [19].

2.3. Photonic Band Crystals Lasers (PBC)

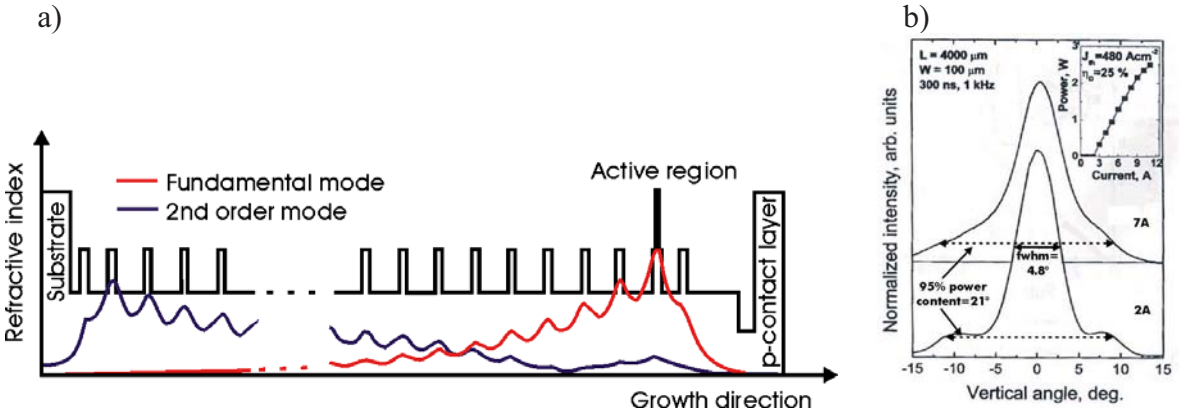

Figure 2.5. (a) The refractive index distribution of the PBC structure with the fundamental and second order mode patterns. (b) Vertical far-field profiles measured at different current levels. Redrawn from [20-21].

This type of structures has its origin in the passive waveguide structures. Lasers based on the photonic band crystal concept utilize very wide (10 µm – 30 µm) waveguides with a periodic modulation of the refractive index and a localized optical defect – a feature that violates the index periodicity. By an optical defect one understands a high refractive index layer that is wider or higher than the corresponding layers of the rest of the periods (Bragg reflector concept).

The 'localized optical defect' with an embedded active region causes fundamental mode localization with a strong overlap with the active region. At the same time, the mode is widely expanded through the periodic waveguide with a decaying tail. Simultaneously, the higher order modes are expanded over the entire PBC structure, with a low confinement in the active region, and are effectively channeled into the substrate or absorbed. Examples of the refractive index distribution and the profiles of the fundamental and second order modes are presented in figure 2.5.

Shchukin et al. [22] present a design that exhibits a vertical far-field of 8° (FWHM) and an optical power of 20 W (under short 300 ns-pulse operation) from a 100 µm stripe device that is 1.5 mm long. Gordeev et al. [21] also present a PBC laser with 8° vertical divergence (emission wavelength 660 nm). The design realized as 4 µm ridge waveguide laser with a cavity length of 1.5 mm exhibits 115 mW in CW operation mode and 20 W under short pulse operation. A 980 nm PBC design, processed as 100 µm wide, 2 mm long device, emits 17 W in pulsed operation into a 4.8° vertical far-field angle. A 10 µm ridge device with a cavity length of 1.5 mm delivers 1.3 W optical (however, not kink-free) power in CW operation mode.

Although the lasers based on PBC design exhibit a very narrow vertical angle at FWHM, the angle containing 95% of the optical power is very wide due to side lobes (figure 2.5.b). The vertical far-field pattern is also unstable at higher current levels.

2.4. Tilted Wave Laser (TWL)

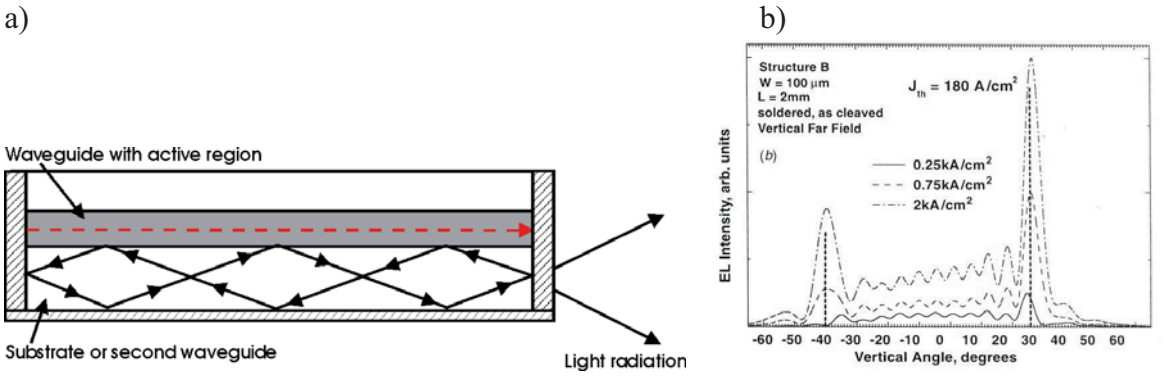

Figure 2.6. (a) Concept of the TWL with light wave propagating in the narrow waveguide and leaky waves in the second large cavity or substrate. (b) The vertical far-field profile at different current levels. Redrawn from [23].

TWL designs are MQW SCH structures that are based on antiguiding and the resonant optical wave coupling phenomenon. The light emitted from the active region is weakly guided into the waveguide and leaks into a second very thick waveguide (10 µm – 30 µm) or into a substrate. The bottom surface of the second vertical optical cavity is usually polished or coated with a highly reflective layer. The structure is designed so that the back-reflected light undergoes constructive (in the case of the fundamental mode) or destructive (for higher